MixDiT: Accelerating Image Diffusion Transformer Inference with Mixed-Precision MX Quantization

Daeun Kim, Jinwoo Hwang, Changhun Oh, *Member, IEEE*, Jongse Park, *Senior Member, IEEE*

***Abstract*—Diffusion Transformer (DiT) has driven significant progress in image generation tasks. However, DiT inferencing is notoriously compute-intensive and incurs long latency even on datacenter-scale GPUs, primarily due to its iterative nature and heavy reliance on GEMM operations inherent to its encoder-based structure. To address the challenge, prior work has explored quantization, but achieving low-precision quantization for DiT inferencing with both high accuracy and substantial speedup remains an open problem. To this end, this paper proposes MixDiT, an algorithm-hardware co-designed acceleration solution that exploits mixed Microscaling (MX) formats to quantize DiT activation values. MixDiT quantizes the DiT activation tensors by selectively applying higher precision to magnitude-based outliers, which produce mixed-precision GEMM operations. To achieve tangible speedup from the mixed-precision arithmetic, we design a MixDiT accelerator that enables precision-flexible multiplications and efficient MX precision conversions. Our experimental results show that MixDiT delivers a speedup of 2.10–5.32× over RTX 3090, with no loss in FID.**

***Index Terms*—Diffusion transformer (DiT), Image generation, Quantization, Microscaling (MX), Acceleration**

I. Introduction

RECENT breakthroughs in diffusion models have sparked a paradigm shift in image synthesis by enabling more stable and high-fidelity generation. A key contributor to this shift is the integration of transformers into diffusion frameworks [1], [4], [10], also known as **Di**ffusion **T**ransformers (*DiT*), building upon their proven success in both language and vision tasks. Figure 1 illustrates the denoising process of diffusion transformer model. Random noise is iteratively and progressively denoised, ultimately resulting in a clear image. This denoising process necessitates repetitive transformer computations, which result in a notably slow inference process. To address this challenge, several recent studies [5]–[7], [12]–[14] have explored quantization to accelerate diffusion models. However, studies for DiT [5]–[7] have struggled to enable quantization for *activations*.

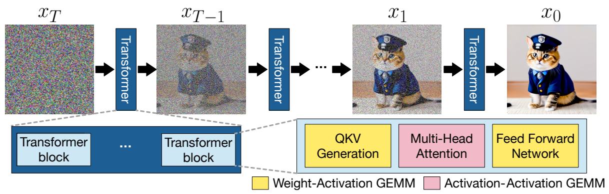

Fig. 1. Denoising process of image generation diffusion with total timestep T and architecture of diffusion transformer.

Rather disjointly, microscaling formats (MX) [9], [11] are emerging as a promising approach for quantization. With its accuracy and hardware efficiency, MX has been standardized by Open Compute Project [11], led by industry giants, and supported on NVIDIA Blackwell GPUs [15]. Although MX has shown effectiveness across various workloads, such as CNNs and LLMs, it remains unexplored in diffusion transformers. In this study, we propose MixDiT, an algorithm-hardware co-designed solution that leverages MX for low-precision quantization in diffusion transformers and introduces a specialized hardware architecture to support mixed-precision computation efficiently. Our contributions are as follows: (1) magnitude-based mixed-precision MX quantization for aggressively low precision while preserving generation quality loss, (2) hyperparameter determination algorithm for mixed-precision thresholding, and (3) precision-flexible MX-supporting accelerator architecture. Our experiments showcase that MixDiT achieves a latency speedup of 2.10× to 5.32× compared to NVIDIA RTX 3090, with no quality degradation in FID.

II. Background and Motivation

A. Image Diffusion Transformer

DiTs employ an encoder-based architecture, comprising Query-Key-Value (QKV) generation, multi-head attention layers, and feedforward networks (FFN). Iterative inferences of these layers incur high latency, even on datacenter-level GPUs. For instance, we observe that Stable Diffusion 3 takes 18.75 seconds for generating a 1,024×1,024 image on RTX-3090.

B. Quantization for Improving Performance

Quantization for DiT. Quantization is a technique that converts floating-point representations into low-precision formats, which helps reduce the memory footprint and improve the computation efficiency. Several prior works [5]–[7] have explored the use of quantization for DiTs. These studies typically use integer (INT) quantization, applying 4-bit for weights, while retaining 8-bit for activations, which limits speedup.

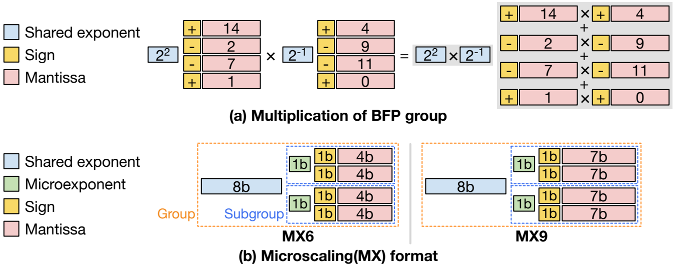

(a) Multiplication of BFP group

(b) Microscaling(MX) format

Fig. 2. Block floating point and microscaling (MX) formats. While our design uses a group size of 16, the illustration depicts a group size of 4 for clarity.

Manuscript received February 27, 2025; revised April 7, 2025. This work was supported by Institute of Information & communications Technology Planning & Evaluation (IITP) (No.2018-0-00503, 33%), ITRC(Information Technology Research Center) grant funded by the Korea government(MSIT) (IITP-2025-RS-2020-II201795, 33%), and National Research Foundation of Korea(NRF) grant funded by the Korea government(MSIT) (RS-2024-00342148, 33%). *(Corresponding author: Jongse Park.)*

The authors are with the School of Computing, Graduate School of AI Semiconductor, Korea Advanced Institute of Science and Technology, Daejeon 34141, South Korea (e-mail: dekim@casys.kaist.ac.kr; jwhwang@casys.kaist.ac.kr; choh@casys.kaist.ac.kr; jspark@casys.kaist.ac.kr)

TABLE I
IMAGE QUALITY AFTER APPLYING MX TO STABLE DIFFUSION 3

Method	Precision (W/A)	FID in COCO-1k (↓)
FP	16/16	74.07
MX	9/9	72.98
	6/9	71.88
	9/6	203.37
	6/6	199.78

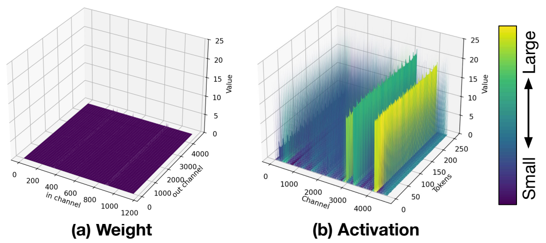

Fig. 3. Magnitude distributions of weights and activations in DiT-XL-256.

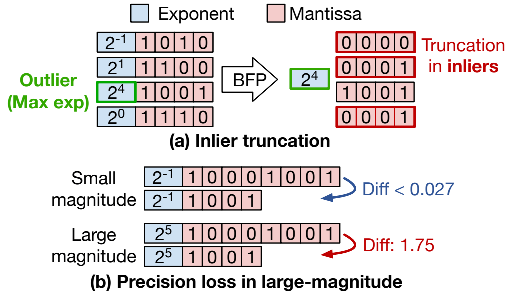

Fig. 4. Impact of large-magnitude values on MX quantization degradation.

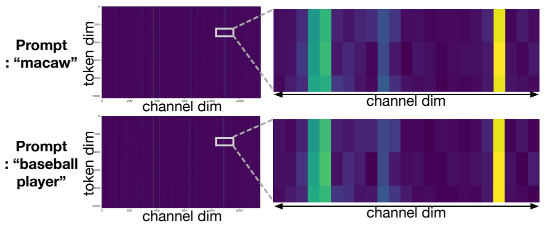

Fig. 5. Observation of linear layer activation's value magnitude in DiT-XL-512. The colors mean same with Fig. 3.

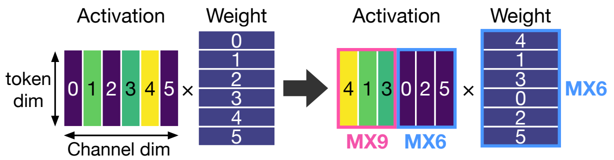

Fig. 6. Channel-wise reordering and mixed precision in linear layer. The colors mean same with Fig. 3.

Microscaling (MX) format. Block floating point (BFP) is one of the low-precision formats that has gained attention for balancing accuracy and computational efficiency. Figure 2(a) shows how BFP multiplication operates. Unlike conventional floating point, BFP simplifies multiplication by grouping values that share an exponent. Microscaling (MX) format [9], [11] is a variant of BFP, as shown in Figure 2(b). MX has demonstrated potential in LLMs but has not yet been explored for DiTs. This work first characterizes the challenges of applying MX to DiT-based models and then leverages these insights to develop *mixed-precision* MX quantization for DiTs.

C. Challenges of Applying MX formats to DiT

Activation sensitivity to low precision. Table I presents the image quality (FID; lower is better) after applying the MX format to Stable Diffusion 3. Applying MX6 to the weights while using MX9 for the activations preserves image quality comparable to FP16, whereas applying MX6 to both weights and activations causes a noticable degradation in image quality. This is due to the value distribution of DiTs. Figure 3 illustrates the magnitude distribution of values in the weight and activation matrices, revealing more pronounced outliers in the activation matrix. These outliers in activations significantly contribute to degradation.

Source of quality degradation. Figure 4 illustrates two primary ways in which large-magnitude values degrade quality. First, inliers within the same group as outliers are truncated because the shared group exponent is set to the largest exponent in the group, leading to precision loss in smaller values. Second, large-magnitude values experience significant quantization error when represented with a 4-bit mantissa, whereas small-magnitude values remain more precise. This work proposes a mixed-precision approach to mitigate these degradations caused by large-magnitude values.

III. DESIGN

This section describes the MX-based mixed-precision quantization scheme and the MixDiT accelerator architecture.

A. Magnitude-based Mixed-Precision MX Quantization

Mixed-precision quantization for linear layers. Figure 5 reports that large-magnitude values concentrate in specific channels, while outliers consistently appear in the same ones regardless of the prompt [5]. Given the observation, we propose a mixed-precision quantization scheme for linear layers, utilizing a channel-wise reordering technique as shown in Figure 6. MixDiT first reorders channels according to their average magnitude, clustering outliers and inliers together to prevent the inlier truncation caused by outliers within the same group. It then reorders weight channels following the same order as the activation channels. After reordering, MixDiT quantizes activation channels with large-magnitude values using high precision (MX9), while applying low precision (MX6) to channels with small-magnitude values and weight matrices. The proportion of activation channels quantized with MX9 is controlled by a hyperparameter, p_1, whose its determination mechanism will be discussed in Section III-B.

Mixed-precision quantization for attention layers. The attention layer, performing activation-activation multiplication, requires a different approach. Figure 7 delineates the scheme. In multi-head attention, each head independently performs the $Q \times K^T$ and $Softmax \times V$ operations. Unlike the linear layer, where outliers are present at the channel level, the attention layer exhibits them at the head level. Analyzing 1,000 COCO prompts, we observed that as in channels in the linear layer, large-magnitude heads remain consistent across various inputs, allowing offline identification. In our head-wise mixed-precision design, heads with large average magnitudes are quantized with MX9, while those with small magnitudes use MX6. As with the linear layer, the proportion of heads

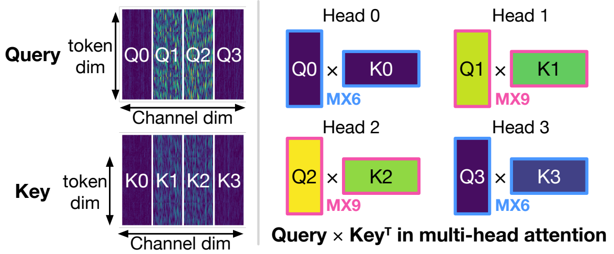

Fig. 7. Head-wise mixed precision in multi-head attention layer. The colors mean same with Fig. 3.

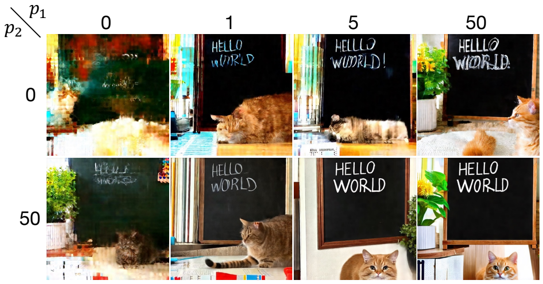

Fig. 8. Image quality-latency tradeoff according to the hyperparameter. Input prompt: "hello world" written on the blackboard and a cat.

quantized with MX9 is controlled by a hyperparameter, p_2.

B. Offline Hyperparameter Determination

Importance of the hyperparameters. Figure 8 shows the quality-latency tradeoff according to the hyperparameter p_1 and p_2. As the p_1 and p_2 increase, a larger portion of the values are quantized with high precision, leading to improved image quality. However, this comes at the cost of increased latency due to the high-precision computations. Additionally, the optimal values of p_1 and p_2 vary across models, while their dependence on data remains marginal.

Hyperparameter determination algorithm. Inspired by these insights, we design an offline hyperparameter determination algorithm. MixDiT sweeps through possible p_1 and p_2 candidates, generating 64 images for each parameter configuration. Then, the algorithm determines p_1 and p_2 by jointly considering (1) the quality of the generated images (measured by FID), and (2) the latency in the hardware. More specifically, we select (p_1, p_2) with minimum $FID \times latency^{\alpha}$. While we empirically set α to 0.15 by default, it can be adjusted to prioritize quality or latency. A higher α emphasizes shorter latency, while a lower α prioritizes higher quality.

C. MixDiT Accelerator Architecture

Architecture for precision-flexible MX quantization support. Figure 9 presents an overview of MixDiT architecture. The accelerator is centered around systolic arrays, which are attached with a reordering controller and an MX converter. Systolic arrays perform computations by fetching the input and weight matrices, pre-ordered in MX format, from off-chip memory. After the computation, the reordering controller selects the appropriate output matrix channels from each bank of the output buffer. For the reordering, the controller maintains a table that specifies the required channel order for each layer and timestep. It forwards these channels in the required order to MX converter. The MX converter then groups and converts the reordered matrix into MX format before storing it in off-chip memory. The MX converter is composed of combinational logic, resulting in negligible latency. The accelerator components operate in a pipelined manner, and the latencies of reordering controller and MX converter are effectively hidden by the significantly larger latency of the systolic array.

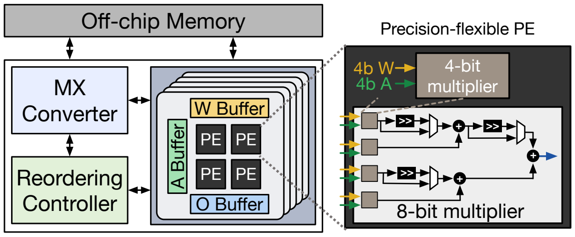

Fig. 9. MixDiT accelerator architecture, built around a systolic array with an MX converter and reordering controller for precision-flexible MX processing.

TABLE II
HARDWARE CONFIGURATIONS

Systolic array size	16x16 PEs	Memory bandwidth	936GB/s
# of systolic arrays	1024	On-chip memory	28MB
Frequency	500 MHz	Peak perf.(MX9)	262 TOPS

MX systolic array. Our mixed precision technique handles MX6×MX9 (for linear layers), MX9×MX9 (for attention layers), and MX6×MX6 operations. The processing elements in the systolic array should support these three types of multiplication. We adopted precision-flexible processing element for MX operations proposed in DaCapo [2]. This PE has four 4-bit multipliers that can do the dot product of the 4-bit mantissa. Therefore, when the group size is 16, MX6×MX6, which needs 4-bit mantissa multiplication, takes 4 cycles per group dot product. MX6×MX9 and MX9×MX9 need 8-bit mantissa multiplication. The outputs of the four 4-bit multipliers mentioned above become one 8-bit multiplier output. Therefore, it takes 16 cycles per group dot product.

IV. METHODOLOGY

Models and datasets. For evaluation, we use DiT-XL [3], Pixart-Σ [4], and Stable Diffusion 3 (SD3) [1]. We denote the generated image resolution by appending $\{256, 512, 1024\}$ to the model name. We use the default settings for the guidance scale of 4.0 and 5.0 for DiT-XL and Stable Diffusion 3, respectively. We perform inference for 25 timesteps across all models. To evaluate the quality, we employ ImageNet-val-5k for DiT-XL, and MS COCO-1k for Pixart-Σ and SD3. We adopt three image quality metrics: fidelity with Frechet Inception Distance (FID), diversity with Inception Score (IS), and prompt alignment with CLIP Score.

Baselines. We employ Q-DiT [5] and ViDiT-Q [7] as quality baselines, both of which are prior works using INT quantization for diffusion transformers. We set the precision to 6 bits for both weights and activations to demonstrate their limitations in low-precision activation quantization. As speedup baselines, we use the original FP16 model and the ViDiT-Q W8A8 model on RTX 3090. Since ViDiT-Q provides an INT8 model only for Pixart-Σ, we conduct our comparison with ViDiT-Q exclusively on Pixart-Σ.

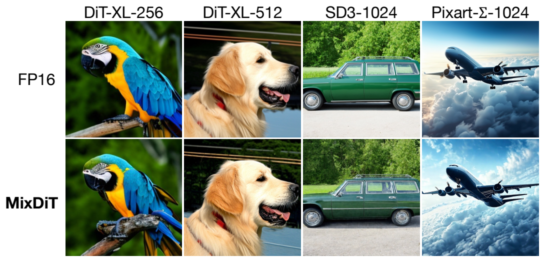

Fig. 10. Images generated by FP16 model and MixDiT.

TABLE III
IMAGE QUALITY EVALUATION

Model (p_1, p_2)	Precision (W/A)	Method	FID↓	IS↑	CLIP score↑
DiT-XL-256 (0, 0)	FP (16/16)	FP16	17.32	231.20	-
	INT (6/6)	Q-DiT	29.27	169.49	-
	MX (6/6)	MX6	67.27	59.99	-
	MX (6/6)	MixDiT	**15.39**	**232.85**	-
DiT-XL-512 (1, 0)	FP (16/16)	FP16	20.55	216.83	-
	INT (6/6)	Q-DiT	**18.04**	209.77	-
	MX (6/6)	MX6	108.70	22.88	-
	MX (6/6)	MixDiT	20.15	**217.77**	-
SD3-1024 (5, 20)	FP (16/16)	FP16	74.07	-	**29.56**
	MX (6/6)	MX6	199.78	-	22.74
	MX (6/6)	MixDiT	**72.48**	-	29.34
Pixart-Σ-1024 (1, 20)	FP (16/16)	FP16	69.96	-	31.34
	INT (6/6)	ViDiT-Q	84.74	-	**31.93**
	MX (6/6)	MX6	71.66	-	31.31
	MX (6/6)	MixDiT	**69.29**	-	31.50

Implementation. We implement the MX quantized model with PyTorch 2.0, Huggingface Diffusers library, and triton language [8]. We develop our accelerator on top of the open-source DaCapo accelerator simulator [2]. Table II shows the hardware configuration for the simulator. We set the group size to 16 and the subgroup size to 2 for MX, and employ a batch size of 1 throughout the experiments.

V. Evaluation

Image quality. Figure 10 visualizes the output image quality of the FP16 model and MixDiT, demonstrating that MixDiT's output image quality matches that of FP16. Table III reports quantitative results for image quality. As Q-DiT and ViDiT-Q are designed to use high activation bitwidths (e.g., INT8/8 or INT4/8), they suffer from poor image quality when using INT6/6 precision. In contrast, our mixed-precision scheme applies MX9 only to activation outliers while using MX6 for the rest, achieving image quality comparable to FP16.

Speedup. Figure 11 reports MixDiT latency speedup compared to the baseline schemes on NVIDIA RTX 3090. When using MX9, our baseline accelerator achieves the same TOPS as the RTX 3090 with INT8. Leveraging the mixed-precision of MX6 and MX9, MixDiT achieves 2.10× to 5.32× speedup compared to the GPU. We observe that only $\leq$5% of activations in linear layers and $\leq$20% of activations in attention layers are quantized with MX9, allowing MixDiT to achieve similar speedups to MX6 while minimizing quality loss. Quantizing most data to MX6 leverages the 4-bit multipliers, which accelerate systolic array computations and serve as the main contributor to the speedup. We notice that larger image generation models see greater improvement, as GEMM computations dominate latency.

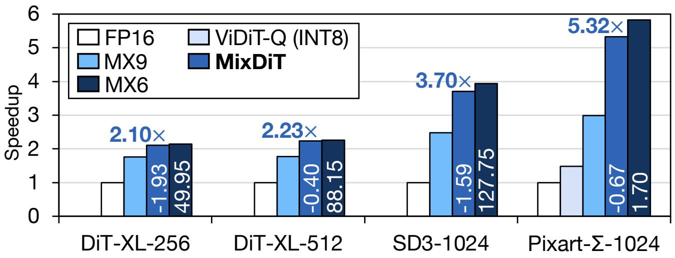

Fig. 11. Latency speedup compared to RTX 3090. The y-axis represents speedup (higher is better), while the numbers inside the bars indicate FID degradation compared to FP16 (lower is better).

VI. Conclusion

This paper presents MixDiT, a mixed-precision quantization framework for accelerating image diffusion transformers using MX formats. Our approach applies higher precision to activation outliers while using low-precision MX computations for the rest, maintaining high image quality. To fully exploit mixed precision, we design a specialized hardware architecture for efficient MX quantization. Combining algorithmic and architectural innovations, MixDiT enables low-precision inference while preserving generation quality, offering a practical solution for efficient diffusion transformer acceleration.

References

[1] Esser, Patrick, et al., "Scaling rectified flow transformers for high-resolution image synthesis," in *Proc. 41st Int. Conf. Mach. Learn.*, 2024, pp. 12606-12633.

[2] Y. Kim et al., "DaCapo: Accelerating Continuous Learning in Autonomous Systems for Video Analytics," in *ACM/IEEE 51st Annu. Int. Symp. Comput. Archit.*, 2024, pp. 1246-1261.

[3] Peebles, William, and Saining Xie., "Scalable diffusion models with transformers," in *Proc. IEEE/CVF Int. Conf. Comput. Vis.*, 2023, pp. 4195-4205.

[4] Chen, Junsong, et al., "Pixart-Σ: Weak-to-strong training of diffusion transformer for 4k text-to-image generation," in *Eur. Conf. Comput. Vis.*, 2025, pp. 74-91.

[5] Chen, Lei, et al., "Q-dit: Accurate post-training quantization for diffusion transformers," 2024, *arXiv:2406.17343*.

[6] Wu, Junyi, et al., "PTQ4DiT: Post-training Quantization for Diffusion Transformers," in *Proc. Int. Conf. Neural Inf. Process. Syst*, 2024, pp. 62732-62755.

[7] Zhao, Tianchen, et al., "Vidit-q: Efficient and accurate quantization of diffusion transformers for image and video generation," 2024, *arXiv:2406.02540*.

[8] Triton Lanauge, "Triton's documentation," 2024. [Online]. Available: https://triton-lang.org

[9] Darvish Rouhani, Bita, et al., "With shared microexponents, a little shifting goes a long way," in *ACM/IEEE 50th Annu. Int. Symp. Comput. Archit.*, 2023, pp. 1-13.

[10] Black-Forest-Labs. "Flux.1," 2024. [Online]. Available: https://blackforestlabs.ai/

[11] Open Compute Project, "OCP Microscaling Formats (MX) Specification," 2023. [Online]. Available: https://www.opencompute.org

[12] LIU, Jun, et al., "FlightVGM: Efficient Video Generation Model Inference with Online Sparsification and Hybrid Precision on FPGAs," in *Proc. 2025 ACM/SIGDA Int. Symp. on Field Program. Gate Arrays*, 2025, pp. 2-13.

[13] Yang, Xinhao, et al., "PARO: Hardware-Software Co-design with Pattern-aware Reorder-based Attention Quantization in Video Generation Models," in *Des. Automat. Conf.*, 2025.

[14] Zhao, Tianchen, et al., "Mixdq: Memory-efficient few-step text-to-image diffusion models with metric-decoupled mixed precision quantization," in *Eur. Conf. Comput. Vis.*, 2024, pp. 285-302.

[15] NVIDIA, "NVIDIA Blackwell Architecture", 2024. [Online]. Available: https://www.nvidia.com/en-us/data-center/technologies/blackwell-architecture/